

Acylated anthocyanin inhibited the formation of heterocyclic amines in hybrid chemical model system and its underlying mechanism

Hui Teng^{a,1}, Yani Mi^{b,1}, Hongting Deng^a, Yuanju He^a, Shunxin Wang^a, Chao Ai^a, Hui Cao^{a,*}, Lei Chen^{a,*}

^a College of Food Science and Technology, Guangdong Ocean University, Guangdong Provincial Key Laboratory of Aquatic Product Processing and Safety, Guangdong Province Engineering Laboratory for Marine Biological Products, Guangdong Provincial Engineering Technology Research Center of Seafood, Key Laboratory of Advanced Processing of Aquatic Product of Guangdong Higher Education Institution, Zhanjiang 524088, China

^b College of Food Science, Fujian Agriculture and Forestry University, Fuzhou 350002, China

ARTICLE INFO

Keywords:

Acylated anthocyanin
Chemical models heterocyclic amine
Inhibition
Enzymatic acylation

ABSTRACT

Enzymatic acylation was employed to synthesize acylated anthocyanin, and a hybrid chemical model system was used for the formation of heterocyclic amines. And the inhibition effect and underline mechanism were investigated by analyzing the variations in important precursors and intermediates. Results confirmed that cyanidin-3-(6-cinnamoyl)-glycosidase (C3(6C)G) with a purity of 98.9% was obtained. HPLC identified seven types of heterocyclic amines (IQ, MeIQx, 4, 8-DimeiqX, Norharman, Harman, PhIP, and AαC) generated in the chemical model. C3(6C)G showed a good concentration-dependent manner for the inhibition effect on most HCAs except for MeIQx and PhIP. It also suppressed the glucose content, showed a dose-dependent manner in creatine/creatinine inhibition, and could scavenge formaldehyde, acetaldehyde, and phenylacetaldehyde. Two potential pathways might be involved: 1. by inhibiting the content of precursors (glucose and creatinine), competing with the formation of amino acids, to suppress HCAs generation; 2 through the removal of reactive carbonyl, reducing its reaction with creatinine.

1. Introduction

Anthocyanins (ACNs) are the most widespread natural pigments in plants, with excellent antioxidant properties, but the poor stability and low bioavailability limit their application in the food industry (Liu, et al., 2020). Acylation modification is an effective method to enhance their stability and improve the solubility to lipid, becoming more suitable for thermal processing (Teng et al., 2022). At present, there are few reports on the practical application of acylated ACNs, but our previous experiment found that acylated ACNs have a significant inhibitory effect on the production of heterocyclic amines (HCAs), which are mutagenic/carcinogenic heterocyclic aromatic compounds produced by high-temperature processing of protein-rich foods (Teng, et al., 2022b).

However, due to the variety of HCAs and the significance of involved processing factors. Besides, the composition of meat products is quite complicated, and unpredictable side reactions are also accompanied in the heating process as well. Thus, it is difficult to explain the formation mechanism of HCAs in details. Up till now, the inhibitory effect of HCAs

is evaluated by food model and chemical model study the (Murkovic, 2004; Quan, et al., 2020). The chemical model system using multiple precursors is able to simulate the formation process of HCAs without causing multiple side reactions, which became an important mean to study the influence of exogenous factors on the formation of HCAs (Murkovic, 2004). The Maillard model of “amino acid + reducing sugar + creatinine” and the pyrolysis system of “amino acid + reducing sugar” are reliable to establish chemical models according to the different formation pathways of aminimidazole type HCAs and amino-carboline type HCAs. Heating the phenylalanine mixture resulted in a higher rate of IQ production (Ishak, et al., 2022). Harman and norharman are mainly derived from the thermal degradation of tryptophan, and their formation is facilitated by the presence of glucose (Wojtowicz, et al., 2015). There are indications that a single model mechanism cannot explore the overall impact of temperature and time on the formation of HCAs (Quan, et al., 2020). Meantime, it was hard to visually represent and compare the performances of different HCAs under the same condition. Until some people found that a mixed system of glucose, creatine

* Corresponding authors.

E-mail addresses: caohui0830@yahoo.com (H. Cao), chenlei841114@hotmail.com (L. Chen).

¹ Authors contributed equally to this work.

(creatinine), phenylalanine, tryptophan, and threonine can solve this problem. However, rarely can find any relative studies on the overall performance of HCAs under different processing conditions in the mixed model.

Therefore, this research employed a hybrid chemical model system consisting of glucose/creatinine(creatinine)/phenylalanine + tryptophan, threonine to produce HCAs and a kinetic study under different temperatures was also employed. The inhibition effect of different concentrations of acylated ACN (cyanidin-3-(6-cinnamoyl)-glycosidase) on the HCAs was investigated in the chemical model. By analyzing the content variations in precursors of HCAs – glucose, creatine/creatinine, amino acids (phenylalanine, tryptophan, threonine) and the active small molecule intermediate products of HCAs – formaldehyde, acetaldehyde, phenylacetaldehyde in the model, inhibition pathway of acylated anthocyanin (C3(6C)G) on HCAs was inspected.

2. Materials and methods

2.1. Materials and reagents

Cyanidin-3-O-glucose (C3G) with a purity of 98 % was ordered from Durst Biotechnology Co., Ltd (Chengdu, China). HCA standards of IQ, MeIQx, 4,8-DiMeIQx, Norharman, Harman, PhIP, and A α C were purchased from Santa Cruz Biotechnology Inc (Santa Cruz, CA, USA). Chromatographic grade of methanol, acetonitrile, ammonium acetate, triethylamine, phosphoric acid, sodium dihydrogen phosphate, disodium hydrogen phosphate and other analytical grade reagents were brought from Sinopharm chemical reagent Co., Ltd (Beijing, China). Methyl cinnamate and 4A molecular sieve of analytical grade were ordered from Maclin Biochemical Technology Co., Ltd (Shanghai, China). Novozym 435 lipase was purchased from Novozymes Biotechnology Co., Ltd (Shenyang, China).

2.2. ACN acylation and purification

The acylation and purification of ACN was proceeded according to a previous study (J. Liu, et al., 2020). Briefly, cyanidin-3-O-glucose (C3G), methyl cinnamate, Novozym435 lipase, and steam flask were dried in a vacuum dryer at 35°C for 24 h. Pyridine was placed in an activated 4A molecular sieve for 48 h for later use. C3G of 20 mg was weighed and put into a distillation flask, then added with 5 mL pyridine, and the flask was placed in an ultrasonic instrument for 2 min to completely dissolve C3G. After that, methyl cinnamate of 1 g and Novozym 435 lipase of 200 mg was added, and the flask was fitted to a rotary evaporator to avoid the light reaction. The acylation was proceeded at 40°C and -0.91 Kpa for 48 h with the rotation speed at 45 r/min.

Semi-preparation liquid phase purification was employed for the purification of acylated anthocyanin (C3(6C)G)s. And the pre-treatment was as follows: the acylated product was transferred to a 50 mL centrifuge tube, and five times the volume of petroleum ether was added for water extraction at 40°C for 10 min. The tube was then centrifuged at 3000 r/min for 10 min, and the supernatant was poured to remove most of the impurities such as methyl cinnamate. After the above extraction and centrifugation steps were repeated twice, an appropriate amount of methanol was added into the centrifuge tube to release C3G and acylated C3G from the enzyme, and the Novozym435 enzyme in the solution was removed by passing through 0.22 μ m filter membrane. Finally, the solution was dehydrated by a constant blow of nitrogen. The semi-prepared liquid chromatography was performed on A BDS HYPERSIL C18 (250 mm x10 mm I.D., 5 μ m) column, and mobile phase A was composed of formic acid aqueous solution (0.1 %, V/V) and mobile phase B was composed of acetonitrile. The elution gradient was 0–20 min, 5–22 % B. 20–40 min, 22–60 % B; 40–60 min, 60–5 % B; 60–65 min, 5 % B. The flow rate was 3.0 mL/min. The column temperature was 30°C. The injection volume was 50 μ L. The detection wavelength was 520 nm and 280 nm.

2.3. Hybrid chemical model system for the formation of HCAs and quantification

The hybrid chemical system was established according to the work reported by (Hui, et al., 2021). The system was consisted of glucose/creatinine/phenylalanine + tryptophan + Threonine model system for HCAs formation: 0.2 mM glucose, 0.4 mM creatine, 0.4 mM creatinine, 0.4 mM phenylalanine, 0.2 mM tryptophan, and 0.4 mM threonine were transferred into a PTFE tube, added with 6 mL of deionized water to dissolve completely, then added with 4 mL diethylene glycol and tighten the lid. The model system was heated in a preheated blast dryer (170, 200, and 230°C) for a certain period of time (10, 20, 30, 40, and 50 min). After that, it was quickly cooled in ice water for half an hour and stored in a refrigerator at 4°C.

Determination of HCAs in the model system: 1 mL reaction solution was put into the test tube, 1 mL of 2 mM sodium hydroxide solution and 4 mL ethyl acetate were added, mixed well in a shaker for 30 min, and allowed to separate different layers by standing at room temperature. The supernatant of 2 mL was collected, dried by nitrogen blowing, re-dissolved in 0.5 mL methanol, filtered by 0.22 μ m filter membrane, and detected by HPLC. HCAs analysis was performed using a high-performance liquid chromatography ultraviolet detector combined with a fluorescence detector (Scott, et al., 2007). The column of TSK-Gel ODS-80 TM (5 μ m, 25 mm \times 4.6 mm.80 A; Tosoh, Tokyo, Japan) was used for the separation and the column temperature was set at 30°C. The mobile phase consisted of solvent A: 0.01 M triethylamine (phosphoric acid adjusted to pH 3.2), solvent B: acetonitrile, and solvent C: 0.01 M triethylamine (phosphoric acid adjusted to pH 3.6). Elution gradient was set as follows: 0 ~ 10 min, 5 %-15 % B; 10 ~ 20 min, 15 %-25 % B; 20–30 min, 25 %-55 % B; 30 ~ 35 min, 55 %-80 % B, flow rate was 1 mL/min. The injection volume was 10 μ L. The UV detection wavelength for IQ, MeIQx, and 4, 8-DiMeIQx was 263 nm. The fluorescence detection wavelength for harman, A α C, and MeA α C was 265/440 nm. The fluorescence detection wavelength for Norharman, PhIP, TRP-P-1, and TRP-P-2 was 265/410 nm.

2.4. Preparation of acylated anthocyanin (C3(6C)G) solution

Acylated anthocyanin (C3(6C)G) solutions in 1.0, 0.5, 0.1, 0 mg/mL were prepared by dissolving the purified acylated anthocyanin (C3(6C)G) powders in diethylene glycol solution. Diethylene glycol of 4 mL as mentioned in the hybrid chemical model system was replaced with 1 mL of the prepared solution of acylated anthocyanin and 3 mL of diethylene glycol. The heating temperature was set at 200°C and the heating time was 30 min.

2.5. Determination of the precursors (glucose, creatine, creatinine, phenylalanine, tryptophan, threonine) contents in HCAs formation

2.5.1. Determination of glucose content

The glucose content was determined according to Serpen and Gökmen (2009) with a slight modification. Preparation of DNS reagent: 315 mg of 3, 5-dinitrosalicylic acid was precisely weighed and transferred into a beaker, added with 50 mL of water, and dissolved in a water bath at 45°C. Sodium hydroxide (NaOH) of 2 g was added into the beaker carefully with a small amount each time. After dissolution, 9.1 g of sodium potassium tartrate tetrahydrate, 250 mg of phenol, 250 mg of anhydrous sodium sulfite, and 30 mL of water were mixed, respectively. Finally, the mixture was transferred into a brown volumetric flask and diluted to 100 mL, and then the DNS solution was stored at room temperature for a week before use.

2.5.2. Determination of creatine and creatinine

HPLC-DAD was employed for the detection and conditions were as follows (Dunnett, et al., 1991; Elbir & Oz, 2020): An InertSustain C18 (150 mm \times 4.6 mm I.D., 5 μ m) column was used. Mobile phase A

consisted of 10 mmol/L sodium dihydrogen phosphate and the buffer solution of disodium hydrogen phosphate (phosphoric acid adjusted to pH 6.2), and mobile phase B consisted of methanol. The elution gradient was as follows, and the column temperature was 30°C. The injection volume was 10 µL. The detection wavelength was 210 nm. The elution gradient was 0–5 min 100 % A, and the flow rate was 0.5 mL/min. 5–7 min 100 % A, flow rate 0.7 mL/min; 7–22 min 30 %A, 70 %B, flow rate 0.7 mL/min; 22–23 min 100 %a, flow rate 0.5 mL/min; 23–30 min 100 %A flow rate of 0.5 mL/min.

2.5.3. Amino acid analysis

According to the method of [Ishak, et al. \(2022\)](#), the content of phenylalanine and tryptophan in the sample was determined. The sample solution was diluted 20 times and filtered with 0.22 µm filter. Standard solutions of phenylalanine and tryptophan with the concentration of 2 mg/mL were mixed 1:1 (V/V) to obtain 1 mg/mL mixed standard solution as a mother solution, and diluted the mother solution into 0.6, 0.5, 0.4, 0.2, 0.1, 0 mg/mL, filtered by 0.22 µm filter, and analyzed by HPLC. The contents of phenylalanine and tryptophan in the samples were calculated.

The determination conditions of HPLC-DAD were as follows: An InertSustain C18 (150 mm x4.6 mm I.D., 5 µm) column was used, mobile phase A was trifluoroacetic acid solution (V/V), mobile phase B was 0.05 % trifluoroacetic acid methanol solution (V/V), and elution gradient was as follows: 0–20 min, 10–100 % B; 20–23 min, 100 % B; 23–25 min, 10 % B; 25–30 min, 10 % B. The flow rate was 1.0 mL/min and the column temperature was set at 30°C. The injection volume was 10 µL and the detection wavelength was 210 nm.

For the determination of threonine was referred to ([Zeng, et al., 2014](#)).

Determination of the intermediates (formaldehyde, acetaldehyde, and phenyl-acetaldehyde) contents in HCAs formation

Determination of formaldehyde and acetaldehyde

The contents of formaldehyde and acetaldehyde were determined by pre-column derivatization of 2, 4-dinitrophenylhydrazine in high performance liquid phase Zhang ([Jeong, et al., 2015](#)). The reaction principle is that 2, 4-dinitrophenylhydrazine (DNPH) reacts with formaldehyde or acetaldehyde and produces stable formaldehyde-2, 4-dinitrophenylhydrazone (formaldehyde-DNPH) and acetaldehyde –2, 4-dinitrophenyl-hydrazone (acetaldehyde-DNPH), respectively, under acidic conditions. Preparation of derivatization reagent: 0.2 g DNPH was placed in a 100 mL brown volumetric flask, added with 0.6 mL phosphoric acid, and diluted to 100 mL with acetonitrile. The sample solution was mixed with the derivative reagent (1:1, v/v), reacted in a water bath at 60°C for 20 min, and then cooled rapidly. The solution of 200 µL was filtered by 0.22 µm membrane and stored at 4°C for analysis.

The HPLC-DAD conditions were as follows: Inertsustain-C18 (150 mm x4.6 mm I.D., 5 µm) column, mobile phase A was chromatographic pure water and mobile phase B was pure acetonitrile. Elution gradient was set as follows: 0–8 min, 30–80 % B; 8–18 min, 80 % B; 18–20 min, 80–30 % B; 20–25 min, 30 % B. The flow rate was 0.5 mL/min and the column temperature was 30°C. The injection volume was 10 µL and the detection wavelength was 360 nm.

2.6.2. Determination of phenylacetaldehyde content

The content of phenylacetaldehyde was determined by the synthesis of 2-substituted benzimidazole derivative (2-Pb) catalyzed by ammonium acetate with the aid of ultrasound ([Cheng, et al., 2008](#)). The working solution was prepared by weighing 0.1 g o-phenylenediamine and 0.1 g ammonium acetate, transferred in a 10 mL volumetric flask, and diluted to a constant volume (10 mL) with acetonitrile. The sample solution of 1 mL was mixed with 0.1 mL of the working solution in a test tube, and allowed to react in an ultrasound bath at 40°C for 3.5 h under dark. After the reaction, the mixture was immediately replaced in a

refrigerator at 4°C to stop the reaction. The mixture was then filtered by 0.22 µm membrane and stored at 4°C for analysis.

The HPLC-DAD detection conditions for the determination of phenylacetaldehyde content were as follows: InertSustain C18 (150 mm x4.6 mm I.D., 5 µm) column, mobile phase A was chromatographic pure water, mobile phase B was pure acetonitrile, elution gradient was set as follows: 0–5 min, 5 % B; 5–10 min, 5–30 % B; 45–70 min, 40–100 % B; 70–74 min, 100–5 % B; 74–80 min, 5 % B. The flow rate was 1 mL/min and the column temperature was 30°C. The injection volume was 10 µL and the detection wavelength was 280 nm.

The data analysis

The experiment was repeated in three sets, and the results were expressed as mean ± standard deviation. SPSS22.0 was used for significance analysis of intra- and intergroup data. SPSS 25.0.0 software was used for one-way ANOVA and origin 2018 software was used for plotting. $P < 0.05$ indicates significant difference.

4. Results and discussions

3.1. Acylation of anthocyanin

[Fig. 1A](#) shows HPLC profile for acylated anthocyanin and the peaks for C3G and acylated ACN was the main compounds with a good separation. LC-MS profile in [Fig. 1B](#) displays that a molecular ion peak [M + H] with a signal peak of 579 appeared, which was the sum of the molecular weight of one cinnamate acyl group (147) and one C3G (449) without hydroxyl group, indicating that the acylation reaction produces a monoacylated C3G. In the secondary mass spectrum ([Fig. 1C](#)), the emergence of a molecular weight of 287 ion fragments, which is obtained by removing a glycosidase from C3G, and the fragments for the molecular weight of 287 gradually increased with the enhancement of collision induced dissociation (CID) as induced by the secondary mass spectrometry. But there were no other ion fragments appeared, which showed that the mother nuclear stability of C3G was strong. Besides, the acylation occurred on glucoside, which was consistent with the study of Yan Zheng ([J. Liu, et al., 2020](#)), and the acylation reaction site catalyzed by Novozym 435 was specific.

Results showed that the conversion rate for enzymatic acylation of cyaniding-3-O-glucose and methyl cinnamate reached 80 %, and the purification process using semi-preparative HPLC increased the purity of acylated C3G to 98.9 %. It was found that the conversion rate in our study was much higher than previous works. [Cruz, et al. \(2017\)](#) early reported a 35 % conversion rate of acylated anthocyanins when C3G was acylated by saturated fatty acids with different carbon chain lengths via enzymatic acylation. Chemical acylation of similar substrates of C3G and saturated fatty acid resulted in a lower conversion rate of 30.8 % ([Zhao, et al., 2016](#)). The reason might be ascribed to the influence of the structures and types of acyl donors, and when esters are chosen as acyl donors, the evaporation of volatile by-products could shift the reaction equilibrium towards synthesis to improve the conversion rate ([Luo, et al., 2022](#)).

3.2. Kinetic curves of 7 types of the HCAs produced in hybrid chemical model under different temperatures

It is well known that chemical modeling system is an effective method to study the influence of different process conditions on the formation of HCAs. The present study employed a hybrid chemical model system consisting of glucose/creatine (creatinine)/phenylalanine + tryptophan + threonine to simulate the formation of HCAs. Seven types of HCAs (IQ, MeIQx, 4, 8-DimeiqX, Norharman, Harman, PhiP, and AαC) were detected by HPLC analysis, indicating the hybrid chemical system was reliable for HCAs simulation. The kinetic curves of the 7 HCAs generated in the hybrid chemical system under different

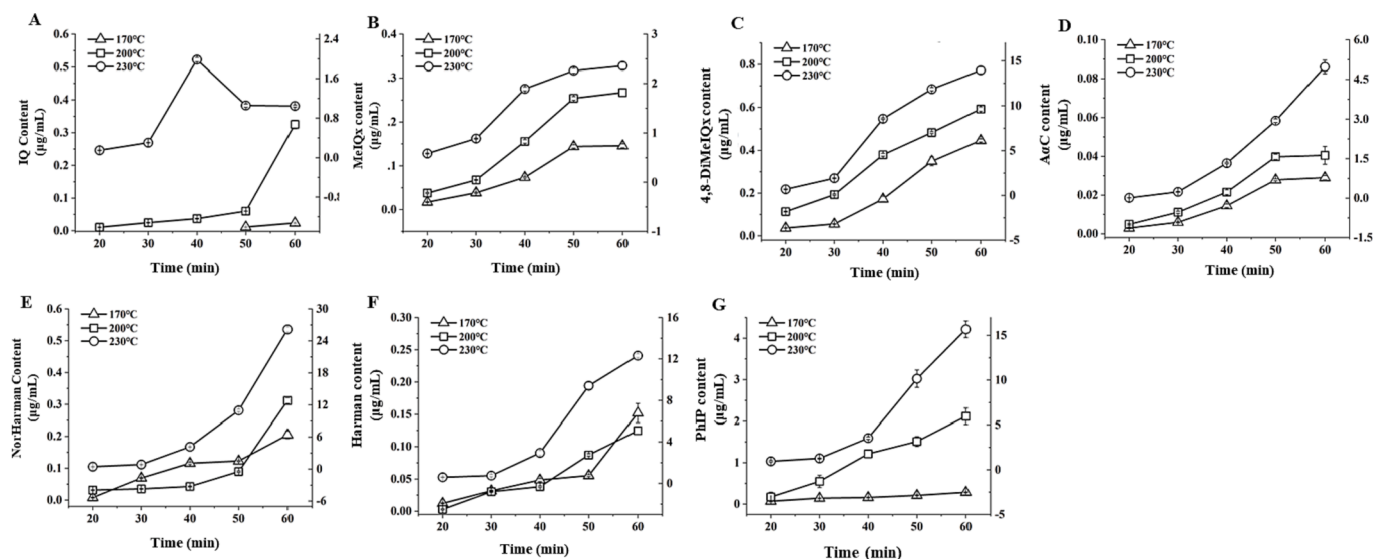


Fig. 1. HPLC profile for acylated anthocyanin at 520 nm (A), and the primary (B) and the secondary (C) mass spectrometry of acylated anthocyanin.

temperatures (170, 200, and 230°C) are shown in Fig. 2(A)-(G). Generally, heating temperature and time were significant variables for the generation of HCAs in the hybrid chemical model. With the prolonged heating time, the contents of 7 HCAs increased. It was worth noting that the IQ was not detected when the time was <50 min under 170°C, and it also showed a quick increase heating at 230°C from 30 to 40 min, but abruptly decreased after that. This might be related to the influence of other components in the system and also due to the degradation of IQ under long-time heating at a high temperature (Chiu & Chen, 2000). Besides, no significant difference between norharman and harman was checked when heating at 170 and 230°C, indicating that the content of β-carbinolines was not affected by heating time under mild temperatures. However, the impact of heating time was magnificent for the formation of HCAs under high-temperature treatment since the slope of the kinetics curve for all 7 HCAs produced at 230°C was higher.

The effect of acylated anthocyanin (C3(6C)G) on HCAs formation in the hybrid chemical model

The inhibition effect of acylated anthocyanin (C3(6C)G) on the formation of HCAs was inspected by supplementing the acylated anthocyanin (C3(6C)G) into the hybrid chemical model and heating at 200°C for 30 min. Table 1 shows the inhibition effects of acylated anthocyanin (C3(6C)G) with different concentrations (0.1 mg/mL, 0.5 mg/mL and 1.0 mg/mL) on the formation of HCAs in the model system. The contents for IQ, MeIQx, 4,8-DiMeIQx, Harman, Norharman, PhIP, and AαC produced in the hybrid chemical model were 24.8 ± 1.44 ng/mL, 286.2 ± 8.52 ng/mL, 233.9 ± 17.02 ng/mL, 36.8 ± 0.99 ng/mL, 36.7 ± 0.31 ng/mL, 101.0 ± 6.48 ng/mL, and 8.1 ± 1.65 ng/mL, respectively. Acylated anthocyanin (C3(6C)G) showed significant inhibitory effects on all of the HCAs ($p < 0.05$), and IQ, 4, 8-diMeIQx, harman, norharman, and AαC represent a concentration-dependent manner on suppressing HCA

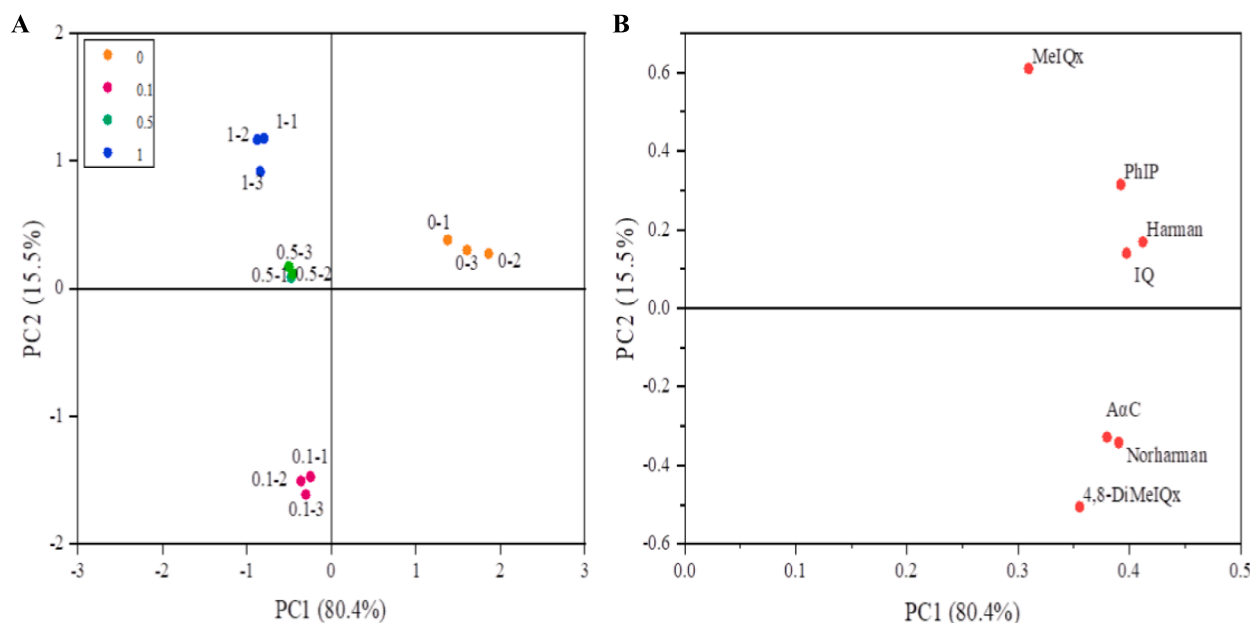


Fig. 2. Kinetic curves of seven types of HCAs generated in chemical model systems at different temperatures (170, 200, 230°C).

Table 1
Effects of different acylated anthocyanin (C3(6C)G) concentration on HCAs content of chemical model system.

Acy-AC (C3(6C)G) conc.	IQ (ng/mL)	MeIQx (ng/mL)	4,8-DiMeIQx (ng/mL)	Norharman (ng/mL)	Harman (ng/mL)	PhIP (ng/mL)	A α C (ng/mL)	Total HCAs (μ g/mL)
0 mg/mL	24.8 \pm 1.44a	286.2 \pm 8.52a	233.9 \pm 17.02a	36.8 \pm 0.99a	36.7 \pm 0.31a	101.0 \pm 6.48a	8.1 \pm 1.65a	0.724 \pm 0.029a
0.1 mg/mL	8.9 \pm 0.57b	199.8 \pm 5.29d	178.5 \pm 9.06b	24 \pm 0.58b	3.2 \pm 0.17b	46.9 \pm 2.4c	5.9 \pm 0.36b	0.465 \pm 0.011b
0.5 mg/mL	13.6 \pm 1.03c	215.6 \pm 3.48c	89.9 \pm 7.94c	12.4 \pm 0.28c	3.0 \pm 0.12b	62.2 \pm 1.64b	4.0 \pm 0.25c	0.400 \pm 0.011c
1 mg/mL	7.3 \pm 0.74d	247.2 \pm 5.81b	20.3 \pm 2.67d	7.2 \pm 0.57d	2.4 \pm 0.11c	53.7 \pm 2.14c	3.0 \pm 0.45c	0.340 \pm 0.009d

formation. The highest inhibition ratio of acylated anthocyanin (C3(6C)G) at 1.0 mg/mL for IQ, 4,8-DiMeIQx, Harman, Norharman, and A α C were 71 %, 91 %, 80 %, 93 %, 63 %, and 53 %, respectively. We also found that acylated anthocyanin (C3(6C)G) was more easily exposed to high temperature and degraded faster in the chemical model system than that happened in the food system, so adding a high concentration of acylated anthocyanin (C3(6C)G) could lead to a higher inhibition effect on HCAs in the hybrid chemical model.

Fig. 3 (A, B) shows the PCA score diagram and load diagram of HCAs in the chemical model system added with different concentrations of acylated anthocyanin (C3(6C)G). The sum of PC1 and PC2 in the figure was 95.9 % (>50 %), which represents the analysis diagram and can explain 95.9 % of the results. The results showed that the PCA model was reliable and valid to reflect HCAs information of the blank group and acylated anthocyanin group. Fig. 3A reflected only the blank group (without acylated anthocyanin (C3(6C)G)) distributed in the second quadrant, which was far from the positions of acylated anthocyanin (C3(6C)G) added groups, indicating a significant difference between the blank and acylated anthocyanin (C3(6C)G) groups ($p < 0.05$). In addition, the medium-dose group (0.5 mg/mL) and the high-dose group (1.0 mg/mL) were all distributed in the first quadrant but not close to each other, while the low-dose group was all in the third quadrant, indicating that the sensitivity of acylated anthocyanin (C3(6C)G) to HCAs was variable with different concentrations of acylated anthocyanin (C3(6C)G). As can be seen from the loading plot, the positions of blank groups in the score plot are similar to these of MeIQx, PhIP, Harman, and IQ in the

loading plot, suggesting that acylated anthocyanin (C3(6C)G) can effectively inhibit these HCAs.

3.4. The effect of acylated anthocyanin (C3(6C)G) on the precursors (glucose, creatine/creatinine, amino acids) of HCAs formation

AIA type HCAs are usually composed of creatine/anhydride, amino acids, and carbohydrates, which are primary constituents of the Maillard reaction. Glucose is a critical precursor of AIAs type HCAs. The generation of HCAs is usually accompanied by the consumption of precursor components, so glucose concentration is an important factor affecting the formation of HCAs. Fig. 4(A) shows the changes of glucose content in the chemical model system after adding different concentrations of acylated anthocyanin (C3(6C)G). The glucose content in the chemical model samples without acylated anthocyanin (C3(6C)G) was 5.076 ± 0.0061 mg/mL, while the glucose content in the samples with acylated anthocyanin (C3(6C)G) was significantly decreased to 0.4592 ± 0.0069 mg/mL, but insignificant difference was observed for different concentrations. Table 1 also confirmed the declined production of AIAs type HCAs in the samples added with acylated anthocyanin (C3(6C)G), indicating that the reduced glucose content led to a decrease in the production of HCAs content.

Fig. 4(B) and (C) show the changes in creatine and creatinine contents in the chemical model system after adding different concentrations of acylated anthocyanin (C3(6C)G). Creatine/creatinine contents in the chemical model significantly decreased with the increase of acylated

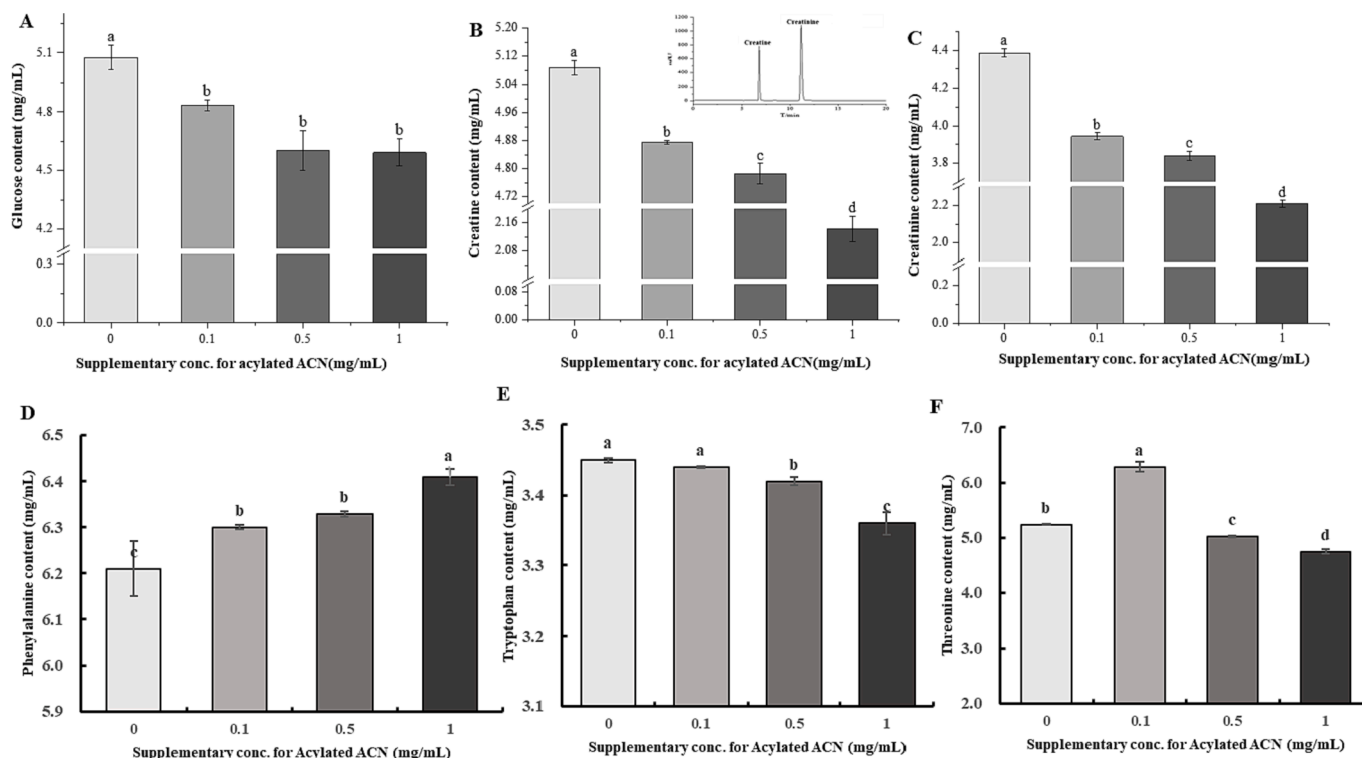


Fig. 3. (A) Scores plot and (B) loadings plot of PCA analysis of HAAs in different acylated anthocyanin (C3(6C)G) addition of chemical model system.

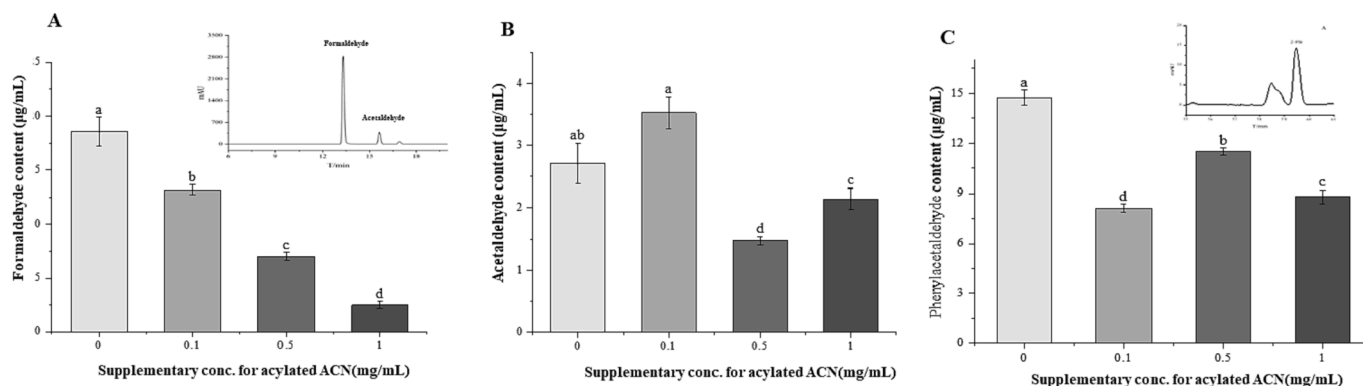


Fig. 4. Changes of the precursors including (A) glucose content, (B) creatinine content, (C) creatinine content, (D) phenylalanine, tryptophan, and threonine contents in chemical model system after adding different concentrations of acylated anthocyanin (C3(6C)G).

anthocyanin (C3(6C)G) concentration ($p < 0.05$). Relative studies have revealed that compounds with electrophilic groups can react with creatinine through enolization, leading to a reduced content of creatinine (Shanmugam et al., 2022). Thus, the super-oxic cation of acylated anthocyanin (C3(6C)G) might be the reason for reducing the content of creatinine.

Phenylalanine is an important precursor of PhIP. Through the Strecker reaction with glucose, phenylalanine degrades to form phenylacetaldehyde and then reacts with creatinine to finally get PhIP. Fig. 4D shows that the content of phenylalanine in the samples with acylated anthocyanin (C3(6C)G) is higher than that in the samples without acylated anthocyanin (C3(6C)G), indicating that acylated anthocyanin (C3(6C)G) can reduce the degradation of phenylalanine in the chemical model system. The effect of acylated anthocyanin (C3(6C)G) on PhIP in Table 1 and creatine/creatinine contents in Fig. 4(B) and (C) confirmed that acylated anthocyanin (C3(6C)G) inhibit PhIP formation via competitive inhibition with phenylalanine to reduce the hydroxylaldehyde condensation reaction between creatine/creatinine and the product of phenylalanine.

Threonine is considered to be another important precursor to provide quinoline (IQ) and quinoxaline (MeIQx, 4, 8-DiMeIQx) type HCAs with pyridine, pyrazine rings, and small aldehydes through the Strecker degradation. Fig. 4(F) displays that threonine content increased when the concentration of acylated ACN (C3(6C)G) was 0.1 mg/mL, but a significant decline occurred with the increased concentration of C3(6C)G to 1.0 mg/mL. This may reflect variations in the inhibition mechanism of acylated anthocyanin (C3(6C)G) in different concentrations for the production of the end products of quinolone and quinoxaline). A low concentration of acylated anthocyanin (C3(6C)G) was primarily through competitive inhibition with threonine to reduce the reaction with other precursors (glucose), inhibiting the formation of PhIP. When the acylated anthocyanin (C3(6C)G) concentration was high (0.5 mg/mL, 1.0 mg/mL), the Threonine content was lower than that of the system without acylated anthocyanin (C3(6C)G), and it decreased with the increase of the concentration. From our previous studies, it is known that acylated anthocyanin (C3(6C)G) has a strong scavenging ability on various free radicals, which is enhanced with the increase in concentration. The free radicals will attack amino acids to produce aldehydes, which in turn act on pyridine or pyrazine rings with creatinine to produce HCAs. Therefore, it can be speculated that the higher concentration of acylated anthocyanin (C3(6C)G) can affect the production of AIAs HCAs mainly by scavenging free radicals.

3.5. The effect of acylated anthocyanin (C3(6C)G) on the intermediate products (Formaldehyde, acetaldehyde, and phenylacetaldehyde) of HCAs formation

According to related literature, formaldehyde was the intermediate

of IQ and MeIQx, and acetaldehyde was the intermediate of 4, 8-DiMeIQx. Meanwhile, Xue, et al. (2020) found that the active carbonyl compound (acetaldehyde) produced by Maillard reaction is the key intermediate in the formation of β -carboline type HCAs. Fig. 5(A) and (B) show the changes in formaldehyde and acetaldehyde contents in the chemical model system after adding different concentrations of acylated anthocyanin (C3(6C)G). It can be seen from the figure that the formaldehyde content in the chemical model samples decreased significantly with the increase of the acylated anthocyanin (C3(6C)G) concentration. The influence of acylated anthocyanin (C3(6C)G) on the variation in acetaldehyde content in chemical model samples was consistent with that observed in the threonine content mentioned earlier.

Phenylacetaldehyde, as a key intermediate of PhIP, is significantly related to its final product PhIP as reported in many studies, which might possibly be due to the aldol condensation with the creatinine is rate-limiting step. Variation of phenylacetaldehyde content in the chemical model system after supplementing different concentrations of acylated anthocyanin (C3(6C)G) is represented in Fig. 5 (C). As expected, the content of phenylacetaldehyde in the acylated anthocyanin (C3(6C)G) group was decreased compared with that in the blank group, which was consistent with the trend of PhIP formation (Table 1), suggesting that the acylated anthocyanin (C3(6C)G) inhibited PhIP formation by scavenging phenylacetaldehyde from the system. The decrease of free radical content leads to the decrease of lipid peroxidation and active carbonyl intermediate of phenyl-acetaldehyde. Combined with the previous studies, it can be determined that another important way of

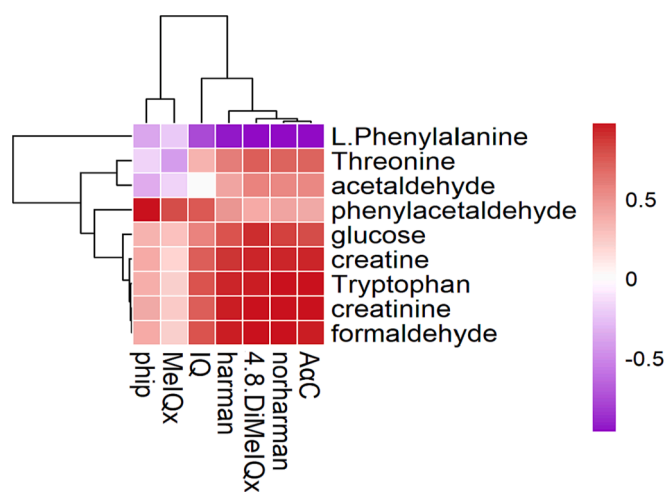


Fig. 5. Changes of the intermediate products (A: formaldehyde, B: acetaldehyde content, and C: phenylacetaldehyde) contents in chemical model system after adding different concentrations of acylated anthocyanin (C3(6C)G).

PhIP inhibition by acylated anthocyanin (C3(6C)G) is by scavenging free radicals in the system. When the acylated anthocyanin (C3(6C)G) concentration was 0.1 mg/mL, the abnormal decrease of phenylacetaldehyde might be affected by other components in the system.

3.6. The potential relationship between HCAs and their precursors/intermediates in chemical model system supplemented with acylated anthocyanin (C3(6C)G)

In order to further study the relationship between HCAs formation and precursors/intermediates, the spearman algorithm was used to study the correlation between HCAs content and related physical and chemical indexes (Fig. 6). The figure shows the positive and negative relationship between different kinds of HCAs in each group and related physical and chemical indexes. Red represents positive correlation, blue represents negative correlation, and the depth of color indicates the strength of correlation.

The Fig. 6 displays that the creatine /creatinine and glucose had a positive relationship with the formation of HCA, which further verified the acylated anthocyanin (C3(6C)G) inhibited precursors of glucose and creatine/creatinine to interfere with their aldol reaction, suppressing the formation of HCAs. Active carbonyls, such as formaldehyde, acetaldehyde, and phenylacetaldehyde, were also positively correlated with most of HCAs contents, suggesting that acylated anthocyanin (C3(6C)G) inhibited the generation of HCAs by scavenging active carbonyls, which might be based on the free radical scavenging ability of acylated anthocyanin (C3(6C)G).

PhIP showed a strong positive correlation with phenylacetaldehyde (Teng, et al., 2019). IQ is negatively correlated with phenylalanine, which is consistent with the study of (Bordas, et al., 2004). This may be related to the similar structure of PhIP and IQ, and the pyridine part of IQ is provided by phenylalanine. The formation of MeIQx is positively correlated with phenylacetaldehyde, but weakly correlated with formaldehyde. At present, there is no evidence that MeIQx formation is necessarily correlated with phenylacetaldehyde. Sha and Liu (2022) added tea polyphenols with different concentrations to mutton, and analyzed the correlation between intermediates and HCAs in the baked mutton cake. She found the correlation between MeIQx and phenylacetaldehyde at 220°C and 250°C was -0.06 and 0.58 , respectively, which might be related to the degradation of phenylacetaldehyde into formaldehyde at high temperatures.

Conclusion

The present study employed a specified enzymatic acylation method to improve the stability of thermal-sensitive anthocyanin (cyaniding-3-O-glucose), and the effect of acylated anthocyanin (C3(6C)G) on the HCAs formation was investigated with a hybrid chemical model system (glucose/creatine (creatinine)/phenylalanine + tryptophan + threonine). Kinetic curves of seven types of HCAs (IQ, MeIQx, 4, 8-DimeiqX, Norharman, Harman, PhIP, and AαC) showed that heating temperature and time were significant variables for HCAs formation. And acylated anthocyanin (C3(6C)G) (0.1, 0.5, and 1.0 mg/mL) showed a good inhibition effect on the formations of HCAs. The inhibition ratio was as high as 93 % for harman formation in the chemical system, except for MeIQx and PhIP, the inhibition effect of HCAs was concentration-dependent on acylated anthocyanin (C3(6C)G). According to the analysis of precursors and intermediates, there was two pathways might be involved to explain the possible inhibition mechanism of acylated anthocyanin (C3(6C)G) on the formation of HCAs. One is to inhibit HCAs by inhibiting the content of precursor (glucose and creatinine/creatine) to compete with precursor amino acids; the other is to inhibit HCAs by eliminating the active carbonyl group and reducing its reaction with creatinine, which is related to the ability of acylated anthocyanin (C3(6C)G) to scavenge free radicals. It was expected that the present study could help to provide a theoretical basis for the application of acylated

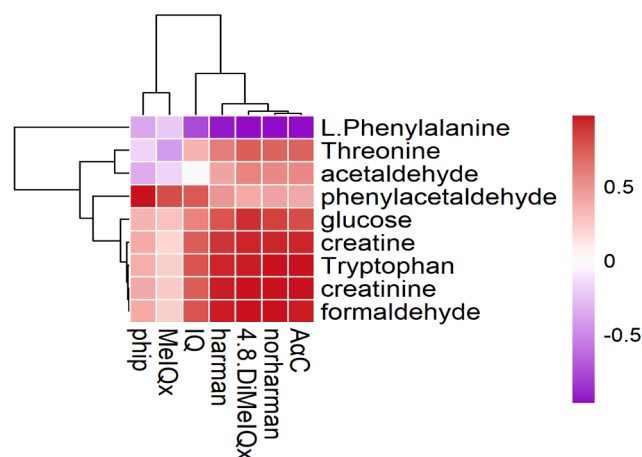


Fig. 6. Heat map of associations between HAAs and their precursors in chemical model sample supplemented with acylated anthocyanin (C3(6C)G).

anthocyanin (C3(6C)G) in the detoxification of HCAs during high-temperature cooking of meat products.

Declaration of Competing Interest

The authors declare that they have no known competing financial interests or personal relationships that could have appeared to influence the work reported in this paper.

Data availability

The data that has been used is confidential.

Acknowledgement

This work is supported by the National Natural Science Foundation of China (NSFC, Grant No. 32072209, 32061160477), the Natural Science Foundation of Guangdong Province (2022A1515010694), China Postdoctoral Science Foundation Funded Project (2020M682073), the Innovative Team Program of High Education of Guangdong Province (2021KCXTD021).

References

- Bordas, M., Moyano, E., Puignou, L., & Galceran, M. T. (2004). Formation and stability of heterocyclic amines in a meat flavour model system. Effect of temperature, time and precursors. *Journal of Chromatography. B, Analytical Technologies in the Biomedical and Life Sciences*, 802(1), 11–17.
- Cheng, K. W., Wong, C. C., Cho, C. K., Chu, I. K., Sze, K. H., Lo, C., ... Wang, M. F. (2008). Trapping of Phenylacetaldehyde as a Key Mechanism Responsible for Naringenin's Inhibitory Activity in Mutagenic 2-Amino-1-methyl-6-phenylimidazo [4,5-b] Pyridine Formation. *Chemical Research in Toxicology*, 21(10), 2026–2034.
- Chiu, C. P., & Chen, B. H. (2000). Stability of heterocyclic amines during heating. *Food Chemistry*, 68(3), 267–272.
- Cruz, L., Guirrares, M., Araujo, P., Evora, A., de Freitas, V., & Mateus, N. (2017). Malvidin 3-Glucoside-Fatty Acid Conjugates: From Hydrophilic toward Novel Lipophilic Derivatives. *Journal of Agricultural and Food Chemistry*, 65(31), 6513–6518.
- Dunnett, M., Harris, R. C., & Orme, C. E. (1991). Reverse-phase ion-pairing high-performance liquid chromatography of phosphocreatine, creatine and creatinine in equine muscle. *Scandinavian Journal of Clinical and Laboratory Investigation*, 51(2), 137–141.
- Elbir, Z., & Oz, F. (2020). Determination of creatine, creatinine, free amino acid and heterocyclic aromatic amine contents of plain beef and chicken juices. *Journal of Food Science and Technology-Mysore*. <https://doi.org/10.1007/s13197-020-04875-8>
- Hui, T., Li, Y., Chen, R., Yang, X., Liu, H., Wang, Z., & Zhang, D. (2021). Formation and Prediction of PhIP, Harman, and Norharman in Chemical Model Systems Containing Epicatechin under Various Reaction Conditions. *Journal of Agricultural and Food Chemistry*, 69(49), 14975–14984.

- Ishak, A. A., Jinap, S., Sukor, R., Sulaiman, R., Abdulmalek, E., & Hasyimah, A. K. N. (2022). Simultaneous kinetics formation of heterocyclic amines and polycyclic aromatic hydrocarbons in phenylalanine model system. *Food Chemistry*, 384.
- Jeong, H. S., Chung, H., Song, S. H., Kim, C. I., Lee, J. G., & Kim, Y. S. (2015). Validation and Determination of the Contents of Acetaldehyde and Formaldehyde in Foods. *Toxicology Research*, 31(3), 273–278.
- Liu, J., Zhuang, Y., Hu, Y., Xue, S., Li, H., Chen, L., & Fei, P. (2020). Improving the color stability and antioxidation activity of blueberry anthocyanins by enzymatic acylation with p-coumaric acid and caffeic acid. *LWT*, 130, Article 109673.
- Liu, J. N., Zhuang, Y. H., Hu, Y. H., Xue, S., Li, H., Chen, L., & Fei, P. (2020). Improving the color stability and antioxidation activity of blueberry anthocyanins by enzymatic acylation with p-coumaric acid and caffeic acid. *LWT-Food Science and Technology*, 130.
- Luo, X., Wang, R., Wang, J., Li, Y., Luo, H., Chen, S., ... Han, Z. (2022). Acylation of Anthocyanins and Their Applications in the Food Industry: Mechanisms and Recent Research Advances. *Foods*, 11(14).
- Murkovic, M. (2004). Formation of heterocyclic aromatic amines in model systems. *Journal of Chromatography. B, Analytical Technologies in the Biomedical and Life Sciences*, 802(1), 3–10.
- Quan, W., Li, Y., Jiao, Y., Xue, C., Liu, G., Wang, Z., ... Chen, J. (2020). Simultaneous generation of acrylamide, beta-carboline heterocyclic amines and advanced glycation ends products in an aqueous Maillard reaction model system. *Food Chemistry*, 332, Article 127387.
- Scott, K. A., Turesky, R. J., Wainman, B. C., & Josephy, P. D. (2007). Hplc/electrospray ionization mass spectrometric analysis of the heterocyclic aromatic amine carcinogen 2-amino-1-methyl-6-phenylimidazo[4,5-b]pyridine in human milk. *Chemical Research in Toxicology*, 20(1), 88–94.
- Serpen, A., & Gökmen, V. (2009). Evaluation of the Maillard reaction in potato crisps by acrylamide, antioxidant capacity and color. *Journal of Food Composition and Analysis*, 22(6), 589–595.
- Sha, L., & Liu, S. S. (2022). Effect of tea polyphenols on the inhibition of heterocyclic aromatic amines in grilled mutton patties. ARTN e16811 *Journal of Food Processing and Preservation*. <https://doi.org/10.1111/jfpp.16811>.
- Teng, H., Chen, Y., Lin, X. J., Lv, Q. Y., Chai, T. T., Wong, F. C., ... Xiao, J. B. (2019). Inhibitory effect of the extract from *Sonchus olearleu* on the formation of carcinogenic heterocyclic aromatic amines during the pork cooking. *Food and Chemical Toxicology*, 129, 138–143.
- Teng, H., Mi, Y., Cao, H., & Chen, L. (2022). Enzymatic acylation of raspberry anthocyanin: Evaluations on its stability and oxidative stress prevention. *Food Chemistry*, 372, Article 130766.
- Teng, H., Mi, Y. N., Cao, H., & Chen, L. (2022). Enzymatic acylation of raspberry anthocyanin: Evaluations on its stability and oxidative stress prevention. *Food Chemistry*, 372.
- Wojtowicz, E., Zawirska-Wojtasiak, R., Przygoński, K., & Mildner-Szkudlarz, S. (2015). Bioactive β -carbolines norharman and harman in traditional and novel raw materials for chicory coffee. *Food Chemistry*, 175, 280–283.
- Xue, C. Y., Chen, Q. C., He, Z. Y., Wang, Z. J., Qin, F., Yang, T. Y., ... Zeng, M. M. (2020). Non-precursors amino acids can inhibit beta-carbolines through free radical scavenging pathways and competitive inhibition in roast beef patties and model food systems. *MEAT SCIENCE*, 169.
- Zeng, M. M., Li, Y., He, Z. Y., Qin, F., & Chen, J. (2014). Effects of Different Precursors on Formation of Heterocyclic Amines of Processed Food by Ultra-high Performance Liquid Chromatography Tandem Mass Spectrometry combined with Principal Component Analysis. *Chinese Journal of Analytical Chemistry*, 42(1), 71–76.
- Zhao, L. Y., Chen, J., Wang, Z. Q., Shen, R. M., Cui, N., & Sun, A. D. (2016). Direct Acylation of Cyanidin-3-Glucoside with Lauric Acid in Blueberry and Its Stability Analysis. *International Journal of Food Properties*, 19(1), 1–12.

Further reading

- May, S., Parry, C., & Parry, L. (2020). Berry chemoprevention: Do berries decrease the window of opportunity for tumorigenesis. *Food Frontiers*, 1(3), 260–275.